A Study on Thermal-Structural Analysis for Shearer Ranging Arm Shell

Chenxu Luo, Zhengtong Han [*], Ye Yuan, Yuanyuan Chen

College of Mechanical and Electrical Engineering, China University of Minging and Technology, Xuzhou Jiangsu 221116,China

Abstract

In order to clear the state of shearer ranging arm shell under different temperature and load, a finite element model of the shell was established by analyzing an actual working condition, and the shell thermal boundary conditions are determined by combining with an actual working condition, then the thermal-structural analysis of the shell was carried out, according to analysis results, in working condition the maximum stress increasing 30.3% and the deformation increasing 94.7%, compared with regardless temperature field, which means that the shell stress and deformation are greatly affected by the thermal load. The loading test result indicates that temperature field attaches the great significance to ranging arm stress and deformation, and the analysis results of thermal-structural model for the shell are better able to reflect the change rule of the shell stress during the actual working process. Besides those, the parallelism error of the bearing axis caused by bearing holes deformation was analyzed. Furthermore, the influence caused by the parallelism error of bearing axis was calculated; its value was 61.5% of the permissible tolerances, which provides a guide for the size accuracy design of the bearing holes of the shell, meaning that the driving performance of the drive system was greatly affected by the shell deformation.

1. Introduction

In order to meet the needs of mine production, cutting power of thin seams shearer has been growing, leading to the thermal output capacity increasing and heat dissipating reducing with the size limit, and mechanical properties of thin seams shearer housing are obviously affected by temperature field. Yuan Ye analyzed the load spectrum of a different drum in different conditions by means of MATLAB, and then obtained the influencing factors of drum load spectrum fluctuation [1]. By the analysis of cutting pieces for cutting pick and the test validation, Gunes Yilmaz N. obtained the prediction models of the cutting force for radial bits by using a multiple regression analysis [2]. Based on the analytical study on the load condition of the shearer cutting section in containing pyrites and thin coal seam using the coupled rigid-flexible model, Zhao Lijuan pointed out some questions such as more deformation for shearer ranging arm shell [3]. As for the present research on heat source, C. Changent held that the following sources of dissipation, i.e., power inputs in the model, are considered pick friction and rolling element bearings, and then obtained thermal resistances which account for conduction and convection by methods of lumped elements [4]. Deng G. conducted a study on gear flash temperature, concluding that the flash rise of

temperature is greatly affected by initial temperature, frictional power loss and contact conditions [5]. Wang Liqin conducted a study on the temperature field of rolling bearing based on tribology and heat transfer and concluded that the extremely small clearance and its bad lubrication were the major factors behind the bearing overheating [6-8]. Mruat Taburdagitan held that torque, rational speed and frictional heat flux were the major factors behind the transient temperature field of pick bearing, based on the study of friction thermal output for spur gear pick surface [9]. Lars Bobach calculated the transient temperature rise of pick bearing surface and obtained the computing method of the pick surface friction coefficient and frictional heat flux density [10].

The study of shearer cutting part load and transmission temperature field that has been taken mostly, but no being considered at this stage, is the influence of a coupled effect between thermal loading and mechanical loading to temperature field and deformation of shearer ranging arm shell, attaching the great significance to working performance of drive system, for instance, bearing holes deformation of shearer ranging arm shell leading to the varying of gears meshing position, causing an increase in the gears mesh error, unequal load distributing between gears pick, and so on [11]. The deformation of ranging arm structure, caused by force and thermal load, gives rise to bearing holes deformation, inevitably following with the

---

[*] Corresponding author. e-mail: xzhlunwen@163.com.

location shift of bearings installed on the bearing hole and the transmission precision problem of shearer ranging arm [12-13]. Therefore, the temperature field and thermal-structural coupling effect of shearer ranging arm shell were analyzed in this study by means of ANSYS, which provides a guide for further optimal design of the thin seams shearer. The parallelism error of bearing axis, caused by bearing holes deformation, was studied in the present study; the influence of gears mesh error caused by parallelism error of bearing axis was also analyzed.

2. The Establishment of the Finite Element Model

Considering the complexity of the geometric model of shearer ranging arm shell, we should import the model framed by the means of three-dimensional software PRO/E into ANSYS. The model is meshed using 20 nodes hexahedron Solid90 unit, which is the high-order element for thermal analysis, having a higher precision and a strong flexibility for irregular shape. Solid90 unit would translate into structure unit Solid 95 in the analysis of thermal-structural coupling [16].

The shearer ranging arm shell is casted entirely, mechanically used for cast steel ZG270-500, whose material properties are shown in Table 1.

Table 1. The mechanical properties of ZG270-500

	Elastic Modulus	Poisson Ratio	Density	Specific Heat Capacity	Thermal Conductivity	Coefficient of Thermal Expansion
Shearer ranging arm shell	1.75E11 Pa	0.3	7800 Kg/m³	460.5 J/Kg·K	31 W/M·K	10E-6 /K

To simplify every shell surface into flat plates, the convective heat-transfer formula for every surface was established using the model of fluid flowing over the flat plate surface [17-18]:

$$h_s = 0.332 \cdot \frac{k}{l} \cdot P_r^{1/3} \cdot R_e^{1/2} \quad \text{Laminar Flow} \tag{1}$$

$$h_s = \left(0.037 R_e^{0.8} - 850\right) \cdot \frac{k}{l} \cdot P_r^{1/3} \quad \text{Turbulent Flow}$$

where $P_r = c_p \rho v / k$ is Prandtl criterion, $R_e = ul/v$ is Reynolds criterion, l is the size dimension, k is thermal-conductivity coefficient, c_p is isobaric heat capacity, ρ is density, v is kinematic viscosity, u is the average speed of fluid.

3. The Analysis of Thermal-Structural Coupling

The sample analysis of thermal and structural mechanics for shearer ranging arm shell can not reflect the practical working conditions, to obtain the influence of thermal load and force load on shearer ranging arm shell. Coupling analysis between thermal field and stress field was carried out.
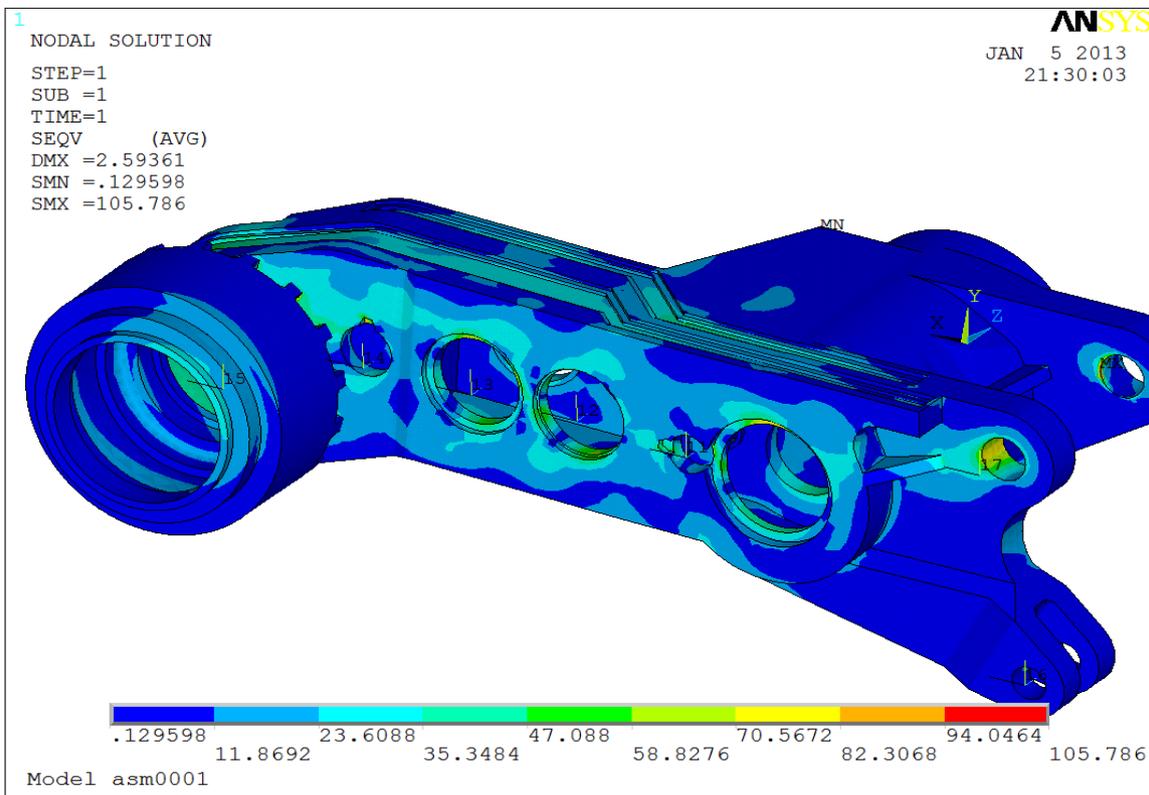
Figure 1. Stress distribution of thermal and structural coupling analysis for ranging arm
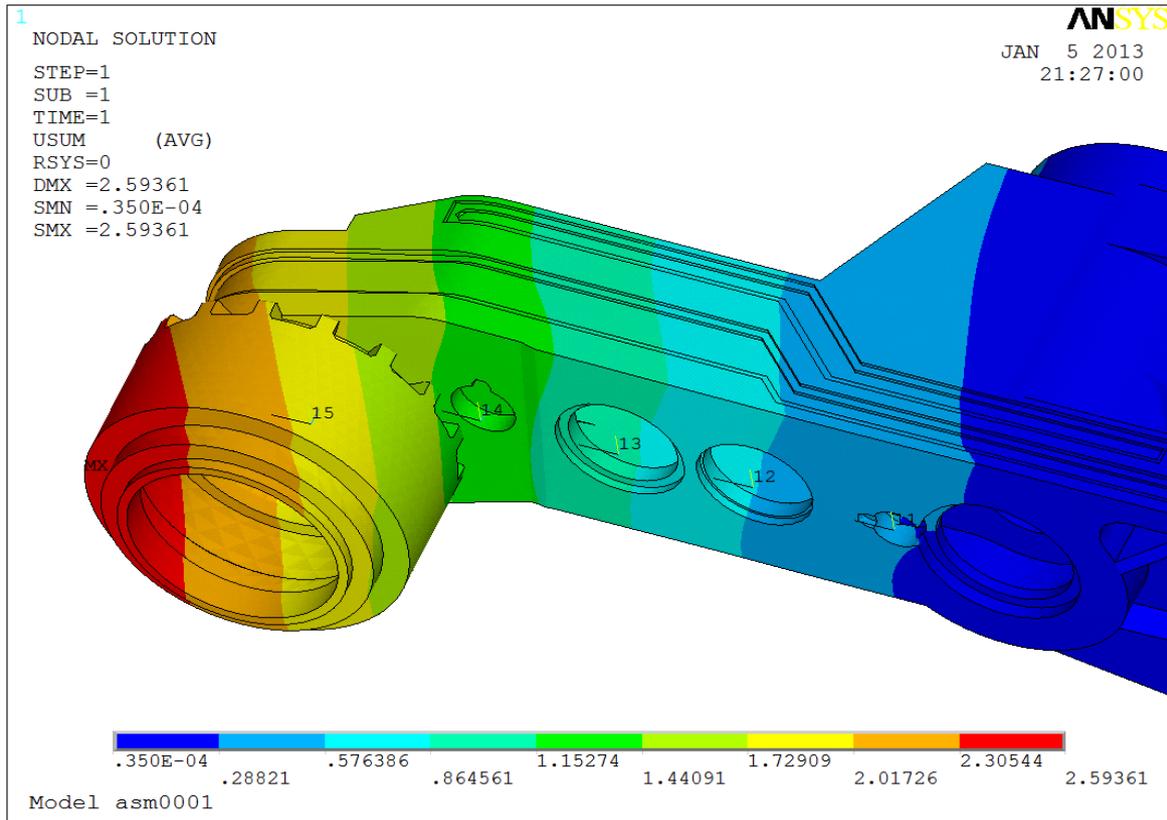
Figure 2. Deformation figure of thermal and structural coupling analysis for ranging arm

Table 2. The temperature and deformation value of bearing hole

Bearing Hole	1	2	3	4	5	6	7	8
Temperature（℃）	69	68	66	59	58	59	59	60
Force-deformation（Mm）	0.1	0.4	0.1	0.9	0.7	0.1	0.7	0.2
Coupled-deflection（Mm）	0.6	2.1	0.7	0.2	0.2	0.7	0.3	0.5

Figures 1 and 2 show the stress and deformation of shearer ranging arm shell after the thermal-structural coupling analysis, respectively. The result indicates that the stress and deformation of shearer ranging arm shell under the thermal load and force load increases when considering the temperature field and produces damage, which would have a negative effect on the performance of the drive system.

Table 2 shows the surrounding temperature and the deformation value from load and coupling of every bearing hole for shearer ranging arm shell. The stress and deformation of each beating hole is bigger than those considered without the temperature field in the thermal-structural coupling analysis, the maximum stress value increasing 10.2% and the deformation increasing 60% ~ 80%, which shows that the thermal stress on the bearing hole is the compressed stress affected by the temperature field, and the stress of beating hole increases by the superposition of force load, in addition that the effect of thermal expansion performs significantly on the beating hole. Among these, the second bearing hole deformation is the biggest, 2.1 mm, mainly affected by its thin surface whose deformation is larger than the other bearing hole after the thermal load and attaches the great significance to clearance and sealing effect of bearings.

4. The Result and Analysis of Shearer Arm Loading Test

In order to verify the validity and the rationality of the finite element analysis and check the consistency of temperature field distribution for shearer ranging arm between in the working process and in the finite element analysis, the loading test bench of shearer arm was established to simulate the working process of shearer ranging arm, and then to determinate the experimental data. The test-bench structure is shown in Figure 3, composed primarily of a driving ranging arm, a determined ranging arm, a hydraulic dynamometer and a supporting component.

The test principle was as follows; the tenon of the driving ranging arm and the determined ranging arm were connected by a sleeve, and the determined ranging arm and the hydraulic dynamometer were connected by a universal coupling. The driving ranging arm drove the transmission system to run, and the determined ranging arm got simulated load by the hydraulic dynamometer, meanwhile every bearing hole temperature of ranging arm was measured every ten minutes using the infrared thermometer.
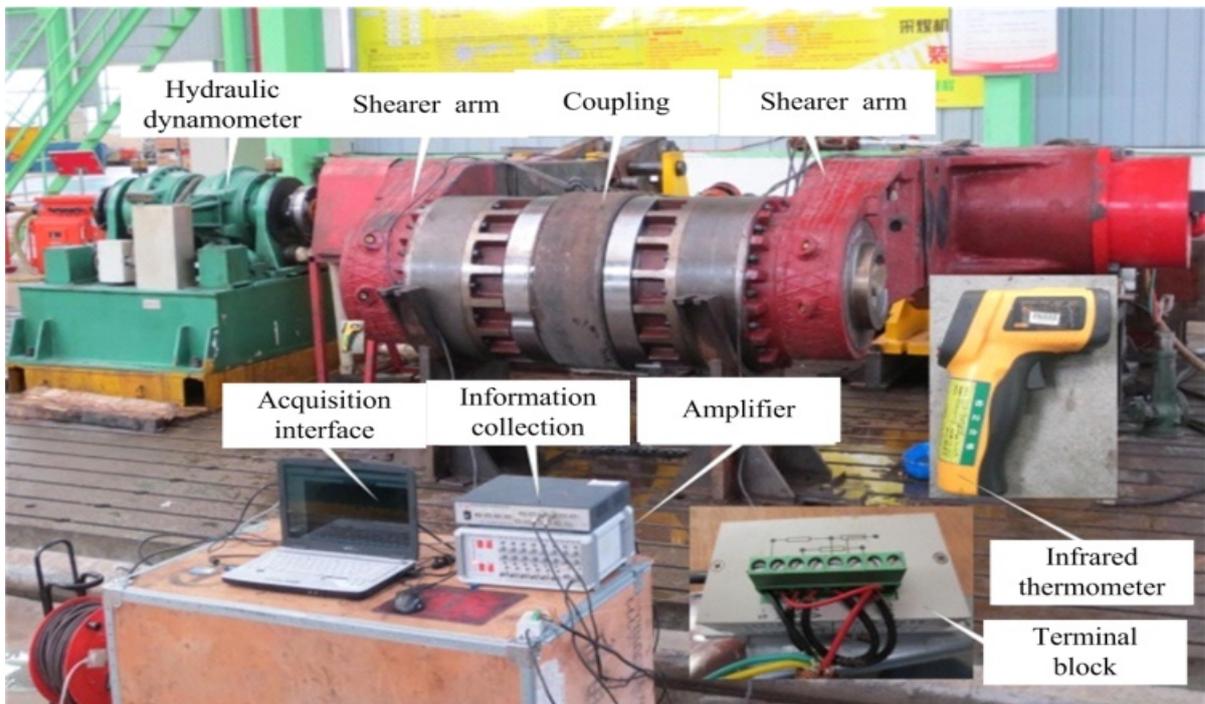
Figure 3. Loading test bench of shearer arm

*4.1. The Load-Thermal Analysis of Ranging Arm*

The rising temperature of each measuring point could be measured after temperature of arm housing increases from room temperature to the thermal equilibrium temperature during the loading process of shearer ranging arm [19].

When the loading test of ranging arm was accomplished after reaching the thermal equilibrium temperature, we could measure the thermal equilibrium temperature of each measuring point using the infrared thermometer and acquire part of the lubricating oil through the drainage port of ranging arm to determine the thermal equilibrium temperature of oil, which is 67.4°C.

The temperature of the bearing hole nodes on coal seam side and mined-out side and the temperature of the top and bottom surface was collected in the finite element steady-state thermal analysis of shearer ranging arm shell, compared with the thermal equilibrium temperature of

shearer ranging arm shell in the loading test, as shown in Figures 4 and 5.

According to the analysis of results (Figures 4 and 5), the consistency of the changing tendency between the finite element analysis temperature and the test temperature on every measured point of shearer ranging arm shell illustrates that the finite element analysis has roughly the same temperature field distribution as that of the test. Comparing between the finite element analysis temperature and the test temperature of every measured point, the test temperature of every measured point, except for the measured point 34 and the measured point 39, is higher than the finite element analysis temperature, whose maximum error rate is 16.9% and average error rate of each measuring point is 10.3%, which indicates that the mathematical model of thermal output and thermal loss and the calculating method of finite element simulation are correct and effective.
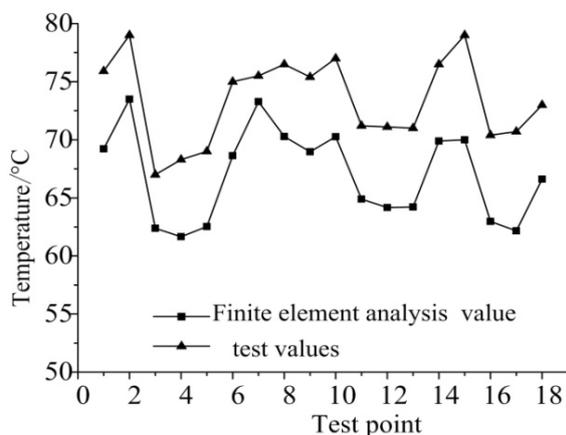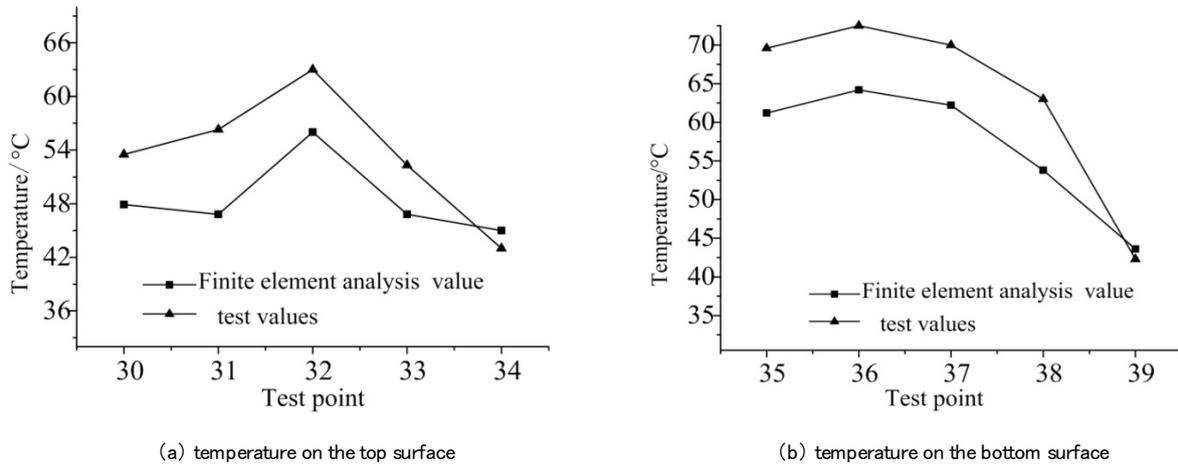

(a) Comparison on coal seam side
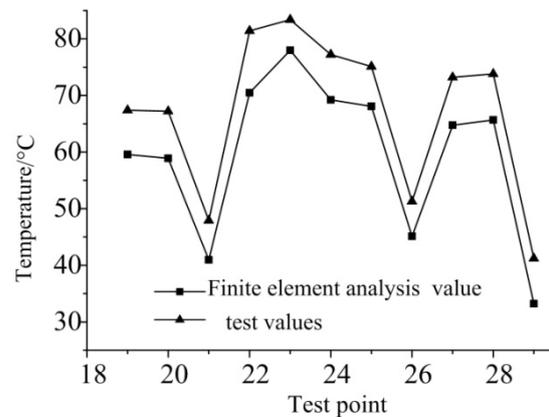
(b) Comparison on mined -out side

Figure 4. Comparison between finite element analysis temperature and test temperature on coal seam side and mined-outside of shearer ranging arm shell

(a) temperature on the top surface   (b) temperature on the bottom surface

Figure 5. Comparison between finite element analysis temperature and test temperature on the top surface and the bottom surface of shearer ranging arm shell

There are a lot of causes of error, mainly including: (1) the model of thermal output and thermal loss is simplified in the finite element analysis, and the heat-transfer coefficient, the heat flux and other parameters is not the same as that under the test; (2) the ambient temperature is set to 11°C and the cooling water temperature is 12.3°C in the test, whereas the ambient temperature is set to 10°C and the cooling water temperature is 15°C in the finite element analysis. If we are able to troubleshoot the influence from the above causes on the analysis and the test, the error between the experimental and the finite element value would be decreasing.

### 4.2. The Stress Analysis of Shearer Ranging Arm Shell

In order to figure out how the temperature field impacts the stress of shearer ranging arm shell, the stress of the first idle shaft hole is measured under ambient temperature and under thermal equilibrium temperature using strain gauges, respectively.

Owing to the different surface thickness of shearer ranging arm shell, the irregular shape, and punching too many holes and grooves, it is difficult to obtain an exact solution to a point of shearer ranging arm shell in theory. Meanwhile limited to testing and measuring facilities, the actual stress value of a point on the shearer ranging arm shell could not be obtained under the determinate load. Therefore, the bridge cannot be calibrated and the measured values are only conducted via a qualitative analysis. The voltage signals measured from the strain bridge represent the stress value of shearer ranging arm shell, to figure out how the stress of the same location on the shearer ranging arm shell is impacted by two different temperature under the same load.
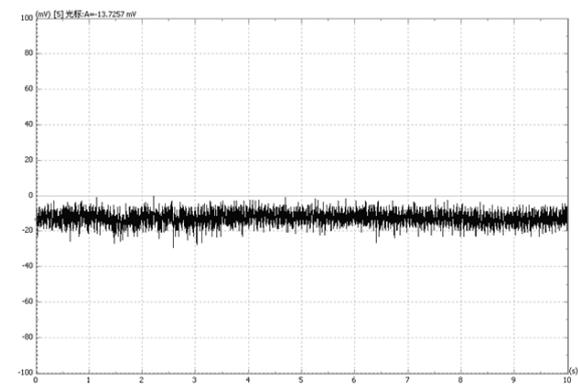
1. The Stress Measurement of Shearer Ranging Arm Shell under the Ambient Temperature

Shearer ranging arm shell temperature is roughly the same as the ambient temperature at the beginning of ranging arm loaded. The voltage signal as a result of stress of the first idle shaft hole on shearer ranging arm shell could be measured using the strain bridge to represent the stress in this condition. The output voltage signal variation

of stress on the first idle shaft hole for shearer ranging arm shell under ambient temperature is shown in Figures 6 and 7.
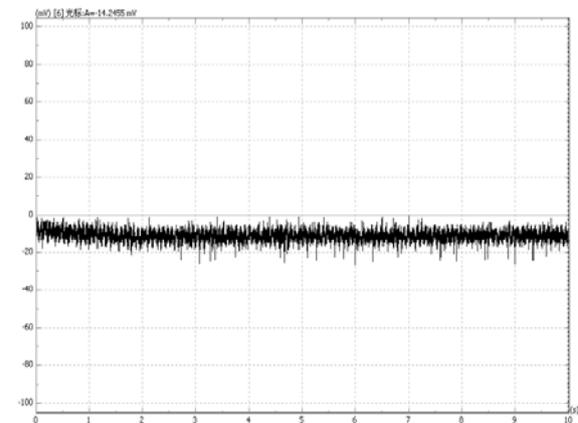
Figure 6. Output voltage signal variation curve of stress under ambient temperature

Figure 7. Output voltage signal variation curve of stress under thermal equilibrium temperature

As shown in the Figure 6, the stress and the deformation of the measured point on the first idle shaft hole nearly stays constant under ambient temperature when the ranging arm achieves stability, and the average voltage is 10.77 mV. Through the analysis of the second chapter, the finite element simulation value of stress measured point is 6.3 MPa.

2. The Stress Measurement of shearer ranging arm shell under Thermal Equilibrium Temperature

When the ranging arm enters into the thermal equilibrium state, the temperature of shearer ranging arm shell is higher and the shearer ranging arm shell is affected by temperature field besides force load. We could measure the output time-varying voltage signal of the first idle shaft hole stress on shearer ranging arm shell under thermal equilibrium temperature using strain gauge bridge, shown in Figure 7.

As shown in Figure 7, reaching the thermal equilibrium temperature, the housing temperature rises and the measured point stress of the first idle shaft hole on shearer ranging arm shell has a constant temperature, whose mean voltage is 12.36 mV against the finite element simulation value is 7.6 MPa.

In conclusion, the stress on the first idle shaft hole attaching train gauges under the ambient temperature and the thermal equilibrium temperature, when conducting loading test for shearer arm on the test bench, were measured. The test results show that the voltage signal on the first idle shaft hole attaching train gauges under the ambient temperature is 10.77 mV and that under the thermal equilibrium temperature is 12.36 mV, which illustrates that the stress of the measured position on shearer ranging arm shell increases by 14.7% when considering the thermal equilibrium temperature field. Extracting the finite element calculation values of shearer ranging arm shell, the housing stress on the measured point under ambient temperature increases 22.2% from the thermal equilibrium temperature. Compared with the test results, the stress error of the measured point in the finite element calculation is 7.5%. The result shows that the temperature field attaches the great significance to the stress variation of shearer ranging arm shell and the analysis results of the thermal-structural coupling model in this thesis could reflect the changing law of the housing stress in the actual working conditions.

5. The Analysis of Influences on Ranging Arm Deformation

1. The Relationship between Housing Bearing Hole Deformation and Its Axis Parallelism

The bearing hole tolerance of ranging arm house includes its parallelism, its roundness, etc., among which the parallelism of bearing holes is the equidistant level between two adjacent bearing holes' center axes of shearer ranging arm shell.

First of all, the thermal-structure coupling for housing bearing hole nodes in the finite element analysis results, including its nodes deformation data in shearer forward direction and the direction towards the roof. Secondly, the displacement value of bearing holes center by calculating the average value of node deformation in all directions could be obtained, as shown in Table 3.
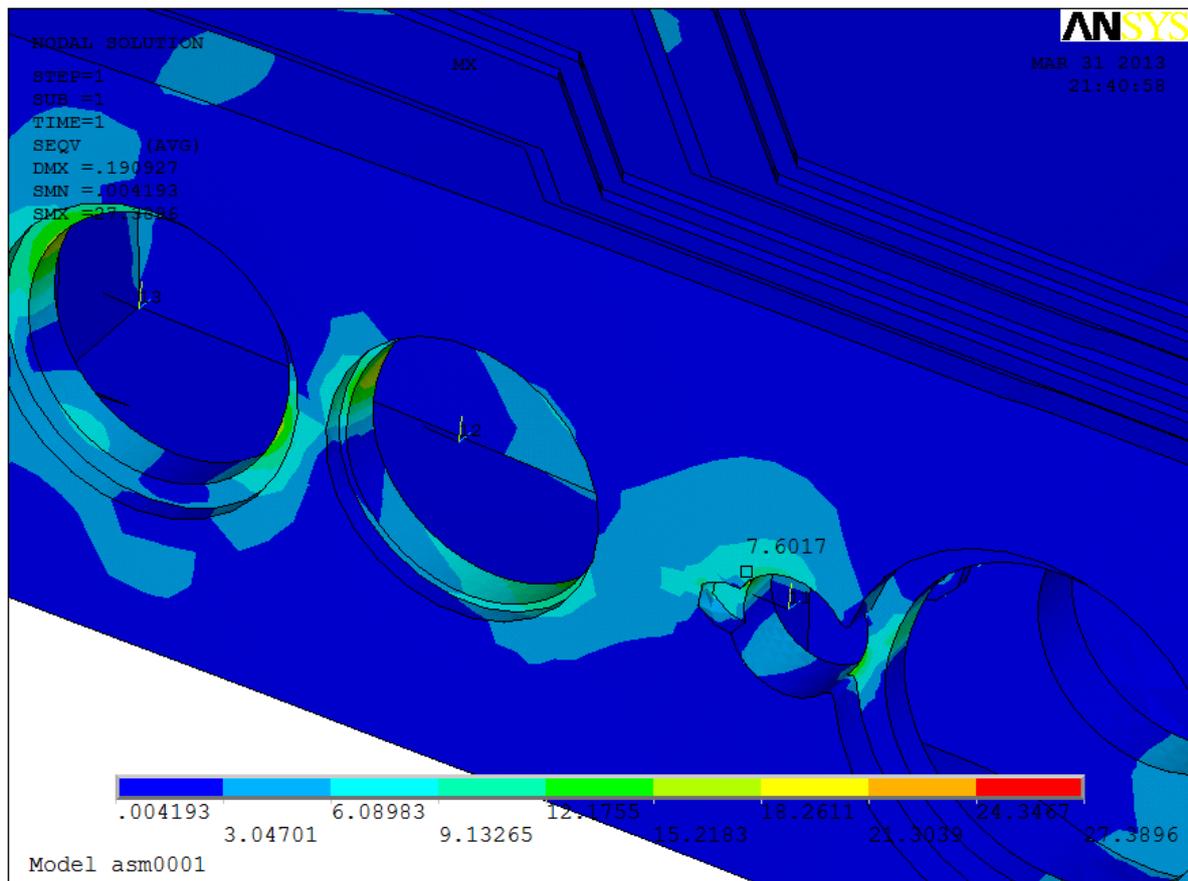

Figure 8. Thermal-Structural coupling stress of shearer ranging arm shell under transmission torque load

Table 3. Displacement Value of Bearing Holes Center

		Coupling Deformation
The First Cutting Shaft Holes	Coal seam side	0.1857
	Mined-out side	0.2890
The First Idle Shaft Holes	Coal seam side	0.3360
	Mined-out side	0.2890
The Second Cutting Shaft Holes	Coal seam side	0.5781
	Mined-out side	0.4725
The Third Cutting Shaft Holes	Coal seam side	0.9231
	Mined-out side	0.7714
The Second Idle Shaft Holes	Coal seam side	1.2897
	Mined-out side	1.1896
The Forth Cutting Shaft Holes	Coal seam side	1.8565
	Mined-out side	1.7733

Table 3 shows that the total deformation values of the largest bearing hole center whose size are 1.95mm, 1.22mm and 1.85mm, respectively. When the ranging arm house is tested under the static load, the thermal load and both, which shows that the static load attaches a greater significance than the thermal load to variation on bearing hole center, and the variability of housing bearing hole center under the thermal-structural coupling load is less than that under the static load. Therefore, the thermal load has a compensating effect on the deformation of bearing hole center on shearer ranging arm shell.

For the relative location relationship between two adjacent bearing hole center lines you can consult Figure 9, i.e., [19-20].

In order to ensure the parallelism of the output shaft, the parallelism error of the second idle shaft axis is calculated using the forth cutting bearing hole axis as the reference element. The parallelism error of the third cutting shaft axis is calculated using the second idle bearing hole axis as the reference element. The parallelism error of the second cutting shaft axis is calculated using the third cutting bearing hole axis as the reference element. The parallelism error of the first idle shaft axis is calculated using the second cutting bearing hole axis as the reference element. The parallelism error of the first cutting shaft axis is calculated using the first idle bearing hole axis as the reference element, as show in Table 4.

Table 4. Parallelism error value of bearing holes axis

Parallelism Error Value	Vertical Direction	Horizontal Direction	Spatial Area
The First Cutting Shaft	0.0143	0.0189	0.0237
The First Idle Shaft	0.0372	0.0172	0.0410
The Second Cutting Shaft	0.0596	0.0232	0.0501
The Third Cutting Shaft	0.0500	0.0242	0.0555
The Second Idle Shaft	0.0572	0.0336	0.0663

Form Table 4, the parallelism error of the second idle bearing hole axis, under the thermal-structural coupling load, is larger than that of the forth cutting bearing hole axis in the horizontal plane, the vertical plane and spatial region, and the parallelism error decreases gradually from lower-speed shaft to high-speed shaft. The result indicates that the hole center deformation of the second idle shaft and the forth cutting shaft are relatively large.

Form Table 3, we notice that the compared bearing holes center displacement data between the second idle shaft and the forth cutting shaft, the deformation of the second idle shaft hole is not the major reason for the larger parallelism error of the second idle shaft, which has two aspects. On the one hand, the forth cutting bearing of shearer ranging arm shell on mined-out side has a large hole diameter and a thin hole surface, as well as the bearing hole is lack of stiffness. On the other hand, the width dimension of shearer ranging arm shell is changeable so much from the second idle bearing hole and the forth cutting bearing hole that the arm housing structure is discontiguous, which is easy to cause deformation; this is shown in Figure 10.
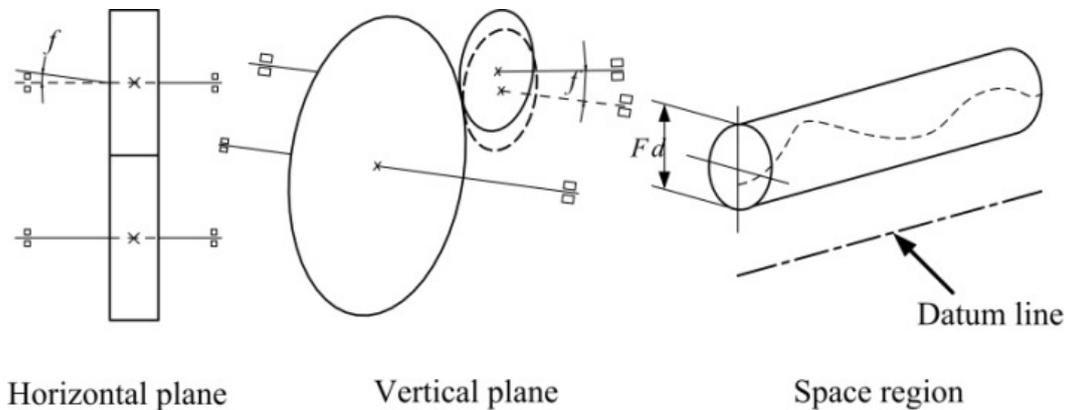
Figure 9. Relative position of lines

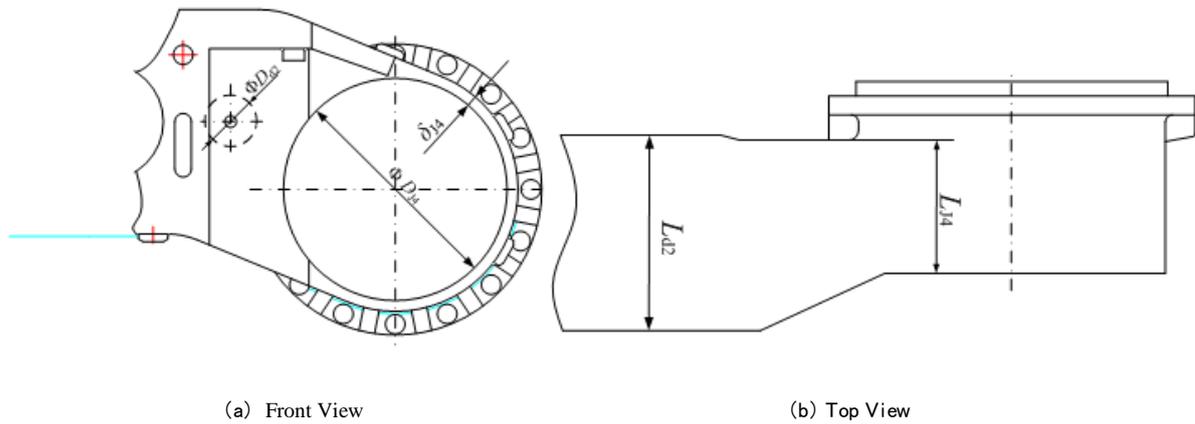(a) Front View   (b) Top View

Figure 10. Local Diagram of shearer ranging arm shell

In Figure 10, the dimension of both bearing hole diameter, the second idle shaft Dd2 and the forth cutting shaft differential DJ4, has a great differential. Ld2 is significantly greater than LJ4, and the dimension of shearer ranging arm shell width has a greater change. It is suggested that bushing with sufficient stiffness be installed in the bearing hole of the forth cutting shaft and to reduce dimensional change of partial shearer ranging arm shell on the lower level as far as possible.

In order to obtain the difference of every bearing hole axis with an ideal situation, the parallelism values of bearing hole centre under the static load were calculated, the thermal load and the thermal-structural coupling load in space area, as shown in Table 5.

Table 5. Parallelism error value of bearing hole centre in space area.

	Coupled effect
The First Cutting Shaft	0.0237
The First Idle Shaft	0.0410
The Second Cutting Shaft	0.0501
The Third Cutting Shaft	0.0555
The Second Idle Shaft	0.0663
The Forth Cutting Shaft	0.0735

From the Table 5, the parallelism error value of bearing hole centre on shearer ranging arm shell in space area is not only one caused by static loadings; the thermal loads were also caused by them. In order to improve the transmission performance of the ranging arm driving system and the parallelism error to conform with the actual working condition, we have to consider the influence of the static loadings and thermal loads on shearer ranging arm shell when the parallelism error of bearing hole centre is calculated.

2. The Influences Analysis of Housing Bearing Hole Deformation on Gear Mesh Error

According to the finite element analysis, the shearer ranging arm shell has a larger deformation under the coupled action of the thermal load and the power load. The maximum parallelism error of bearing hole axis, namely the parallelism error caused by the bearing hole deformation of the forth cutting shaft and the second idle shaft, is used to calculate the influence on gear mesh error.

The second idle gear axis and the forth cutting gear centre point form the horizontal plane, and crossing the second idle gear axis and perpendicular to the gear mesh plane form the meshing vertical plane. the gear axis offset caused by the bearing hole deformation in the meshing horizontal plane and the meshing vertical plane should be calculated, respectively.

Vertical Plane

$$f_{pc} = \frac{\sum \delta_1 - \sum \delta_2}{L} B_z \cos \alpha \qquad (2)$$

Horizontal Plane

$$f_{ps} = \frac{\sum \delta_1 - \sum \delta_2}{L} B_z \sin \alpha \qquad (3)$$

Engaging Plane

$$f_p = \sqrt{f_{pc}^2 + f_{ps}^2} \qquad (4)$$

where $\Sigma\delta_1$ and $\Sigma\delta_2$ represent the total clearance on both ends of bearings, respectively, mm. B_z is the gear pick width, mm. α is the pressure angle of reference circle, $\alpha = 20°$. L is the span at both ends of bearings, mm.

$$\sum \delta_r = \frac{\Delta r}{2} + \frac{\delta_r}{2} + f_{par} + \delta_0 \qquad (5)$$

where, $\Sigma\delta_r$ is the total clearance on both ends of shaft bearings, mm. Δr is radial clearance of bearings, mm. δ_r is tolerance clearance between the shaft and the bearing hole, mm. f_{par} is the parallelism error of the bearing hole, mm. δ_0 is elastic deformation of the bearing, mm. The second idle shaft uses tapered roller bearings, the forth cutting shaft using single-row cylindrical roller bearings, and the radial clearance of bearings is 0.145 mm and 0.13 mm, respectively, the tolerance clearance of bearings holes is 0.016 mm.

The error caused by bearing holes deformation was calculated, and the results are shown in Table 6.

Table 6. Error caused by deformation of bearing hole

	Vertical plane	Horizontal plane	Engaging plane
The Second Idle Shafting	0.0521	0.0189	0.0554
The forth Cutting Shafting	0.0405	0.0147	0.0431

Because the bearing hole deformation direction of the second idle shaft and the forth cutting shaft points into the roof, the gear mesh error of driving gears on the second idle shafts and the forth cutting shafts is:

$$f = f_{pd} - f_{pj} = 0.0544 - 0.0431 = 0.0123 \text{ mm}$$

where f is the gear mesh error of the driving gear in millimeters. f_{pd} is the offset caused by the deformation of the second idle bearing hole in millimeters. f_{pj} is the offset caused by the deformation of the forth cutting bearing hole in millimeters.

The driving system of shearer ranging arm in the present study uses the seventh gear accurate, and the allowable gear mesh error of gears studied here is 0.020 mm by consulting the standard of Precision of cylindrical gear GB10095-88. The gear mesh error caused by the non-parallelism error on account of the housing bearing hole deformation under the thermal-structural coupling load, which is 0.0123 mm, 61.5% of the permissible value. That is to say, during the design process the above-mentioned content should be fully considered.

6. Conclusions

The shearer ranging arm shell is conducted via a thermal-structural analysis by means of ANSYS to obtain stress and deformation under the thermal-structural analysis. The result indicates that the thermal load attaches the great significance to the stress and the deformation of shearer ranging arm shell. The maximum stress on the bearing hole of shearer ranging arm shell under the thermal-structural coupling load is 106 MPa, increasing 30.3%, and the maximum deformation is 2.59 mm, increasing 94.7%, which would affect the transmission performance of the driving system. In order to reduce the thermal effect on shearer ranging arm shell, the force cooling system of the thin seam shearer should be improved.

According to the test research on the temperature field on every surface of ranging arm and the stress of arm housing on the loading test bench of shearer arm, the temperature of each measuring point is measured using the infrared thermometer, whose results indicate that the mathematical model of thermal output and thermal loss and the calculating method of finite element simulation is correct and reliable. The stress of the first idle bearing hole is measured under the thermal equilibrium temperature of shearer ranging arm shell using stress information acquisition system, whose results indicate that temperature field attaches the great significance to ranging arm stress and deformation, and the analysis results of thermal-structural coupling model for shearer ranging arm shell are better in reflecting the change rule of shearer ranging arm shell stress during the actual working process.

Using the deformation data of bearing holes from thermal-structural analysis of shearer ranging arm shell, the parallelism error of bearing axis caused by it was calculated to further analyze the influence of the parallelism error on the gear mesh error. The result indicates that the gear mesh error of the driving system caused by the housing deformation is 61.5% of the permissible tolerances, which provides a guide for the tolerance design of the bearing holes of shearer ranging arm shell.

Acknowledgements

References

[1] Ye Yuan. the simulation analysis and investigation of the drum load spectrum of a shearer. Journal of Shandong University of Science and Technology, Vol.2 (2008), Issue 1, 21-24.

[2] Gunes Yilmaz N,Yurdakul M,Goktan R M. Prediction of radial bit cutting force in high-strength rocks using multiple linear regression analysis. International Journal of Rock Mechanics and Mining Sciences, Vol 1(2007), Issue 44: 960−970.

[3] Zhao Lijuan, Dong Mengmeng. Load problems of working mechanism of the shearer in containing pyrites and thin coal seam. Journal of China Coal Society, Vol. 34(2009)11, 6:840-844.

[4] C.Changent,X.Oviedo Marlot,P.Velex. Power Loss Predictions in Geared Transmissions Using Thermal Networks-Applications to a Six-Speed Manual Gearbox. Journal of Mechanical Design, Vol. 3 (2006) No. 128, 618-625.

[5] Deng G,Kato M.Initial temperature evaluation for flash temperature index of gear tooth[J].Transaction of the ASME,Journal of Tribology, Vol. 117(1995)No. 3, 476-481.

[6] Wang Liqin,Chen Guanci,Gu Le,et al. Study on operating temperature of high-speed cylindrical roller bearings. Journal of Aerospace Power, Vol. 23 (2008) No. 1, 178-183.

[7] Jafar Takabi, M.M. Khonsari. Experimental testing and thermal analysis of ball bearings. Tribology International, Vol. 1(2013)No. 2, 93-103.

[8] Muskat M.. Temperature Behavior of Journal Bearing Systems . Journal of Applied Physics, Vol. 14 (2009) No. 5, 234-244.

[9] Mruat Taburdagitan,Metin Akkok. Determination of surface temperature rise with thermo-elastic analysis of spur gear. Wear, Vol. 261 (2006), No. 1, 656-665.

[10] Lars Bobach, Ronny Beilicke, Dirk Bartel, Ludger Deters. Thermal elastohydrodynamic simulation of involute spur gears incorporating mixed friction. Tribology International, Vol. 48 (2012), No. 1, 191-206.

[11] Zhu Caichao,Lu Bo,Xu Xiangyang,et al.Analysis of heavy duty marine gearbox with thermo elastic coupling. Journal of Ship Mechanics. Vol. 15 (2011) No. 8, 899-805.

[12] Li Runfang.Stiffness Analysis and Modification method for Gear Transmission.Chongqin:Chongqing University Press, 1998.

[13] Pedro M.T. Marques, Carlos M.C.G. Fernandes, et. Power Losses at low speed in a Gearbox Lubricated with Wind

Turbine Gear Oils with special focus on churning losses. Tribology International.Vol 1(2013), No. 2, 1-11.

[14] Zhang Xiaochan. Thermal and Structural Characteristic Analysis and Research of Case for Wind Turbine Generator Gearbox. Dalian University of Technology, (2010), 47-48.

[15] Horejs O, Czech Tech. Thermo-Mechanical Model of Ball Screw With Non-Steady Heat Sources. Theory and Application, Vol. 1 (2007), No. 2, 113-117.

[16] Zhang Zhaohui. Engineering practice of thermal analysis with ANSYS 12.0.Beijing:China Railway Publishing House, (2010) 109-110.

[17] Hekimoglu O Z,Ozdemir L. Effect of angle of wrap on cutting performance of drum shearers and continuous miners. Mining Technology, Vol. 113 (2004) No. 2, 118-122.

[18] Beatriz Lopez-Walle. Dynamic modeling for thermal micro-actuators using thermal networks.Internatonal Journal of Thermal Sciences. Vol.1(2010),No. 11, 2109-2116.

[19] Su Hua, Chen Guoding.Analysis of temperature field and coupled thermal and structure for finger seal. Journal of Aerospace Power, Vol. 24 (2009) No. 1, 196-203.

[20] Guo Ce. Analysis of thermal character istics and thermal deformati on of high-speed spi ndle system in NC precisi on lathe. Journal o f southeast university. Vol. 35 (2005) No. 2, 231-234.

[21] Liu Xuner. The geometric error detection. Beijing:China zhijian publishing house, 2012.